

Optical conductivity of single-layer graphene induced by temporal mass-gap fluctuations

József Zsolt Bernád

Institut für Angewandte Physik, Technische Universität Darmstadt, D-64289, Germany

Institute of Fundamental Sciences and MacDiarmid Institute for Advanced Materials and Nanotechnology, Massey University, Private Bag 11 222, Palmerston North 4442, New Zealand

Abstract

We consider the dynamics of charge carriers in single-layer graphene that are subject to random temporal fluctuations of their mass gap. The optical conductivity is calculated by incorporating the quantum-stochastic time evolution into the standard linear-response (Kubo) theory. We find that, for an intermediate range of frequencies below the average gap size, electron transport is enhanced by fluctuations. At the same time, in the limit of high as well as low frequencies, the conductivity is suppressed as the variance of gap fluctuations increases. In particular, the dc conductivity is always suppressed by a random temporal mass with nonvanishing mean value and vanishes in the zero-temperature limit. Our results are complementary to those obtained recently for static random-gap disorder in finite-size systems.

Keywords: Graphene, Temporal mass-gap fluctuations, Quantum-stochastic time evolution, Generalized Kubo formula, Optical conductivity

1. Introduction

Graphene is a newly accessible nanomaterial [1, 2, 3, 4], consisting of a single sheet of carbon atoms forming a two-dimensional honeycomb lattice. The valence (highest occupied) and conduction (lowest unoccupied) bands of graphene are touching at the \mathbf{K} , $\mathbf{K}' = -\mathbf{K}$ (and equivalent) points in the Brillouin zone and exhibit a conical shape of their dispersion in the vicinity of these special (Dirac) points [5, 6, 7, 8]. Graphene is a promising candidate for applications in future micro- and nanoelectronics due to its excellent mechanical characteristics, scalability to nanometer sizes, and the ability to sustain huge electric currents [9, 10]. Recent experiments have confirmed that the charge carriers in graphene indeed behave like massless Dirac fermions [1, 11].

Although graphene exhibits excellent conducting properties, the absence of an energy gap poses a challenge for realizing conventional semiconductor device operations in this material. A possible way to alleviate this situation is to induce a gap in the electronic spectrum at the Fermi energy by breaking the discrete sublattice symmetry of the honeycomb structure. In recent

Email address: Zsolt.Bernad@physik.tu-darmstadt.de (József Zsolt Bernád)

experiments [12, 13] was reported that hydrogenation of the graphene sheet breaks the sublattice degeneracy. Reversibility of this process enables switching between conducting and insulating regimes of a graphene sample, and spatial addressability should make the fabrication of hybrid conducting-insulating graphene samples possible.

The opening of a uniform gap destroys graphene's metallic state, as the ac (optical) conductivity vanishes for photon energies smaller than the band gap. In real samples, the gap may be random, e.g., because of structural variability in the physical system. For example, the bonds with hydrogen atoms could undergo temporal and spatial variations. To understand this practical issue, and also for more fundamental reasons, studies of *static* random-gap disorder in Dirac-fermion systems have been performed [14, 15, 16, 17], where a staggered potential was considered as a possible model for breaking the sublattice symmetry of the honeycomb lattice. Our work presented here augments these previous investigations by considering the effect of a spatially uniform mass gap that fluctuates *in time*. Besides clarifying the respective nature of temporal and spatial randomness in the mass gap, which is an issue of basic interest, the scenario considered by us would be realized in graphene samples where sublattice-potential-inducing agents are undergoing large-scale random variations. Below we argue that a more general spatio-temporal random variation of a staggered sublattice potential in graphene can be represented, to leading order, by a Markovian model where the low-energy Dirac-fermion theory has a random mass gap described by white-noise fluctuations. We use this model to derive our stochastic equation of motion for the disordered-graphene system and incorporate the nontrivial time evolution into the framework of linear-response theory. Thus a generalized Kubo formula is obtained for the optical conductivity, enabling us to unambiguously determine how electric transport is affected by the mean value and the variance of the fluctuating potential. This is a useful result because the optical conductivity is an experimentally accessible quantity [19, 20, 21, 22] that depends strongly on the electronic properties of the material. In particular, it can be used to determine the size of a band gap [23] since transport is suppressed for photon energies smaller than the gap. We find that the dc conductivity at finite temperature is monotonously decreasing as a function of the variance of mass-gap fluctuations. However, for an intermediate range of frequency below the cut-off equivalent to the average gap, fluctuations *enhance* the conductivity. This observation should be contrasted with the related increase of the conductivity with variance of *static* mass-gap fluctuations in graphene samples of finite size [15, 17].

The remainder of this paper is organized as follows. Our theoretical method is outlined in the following Sec. 2, where a generalized linear-response formula for the conductivity of a system subject to random temporal fluctuations is derived. Results obtained from application of this formalism to randomly gapped graphene are presented in Sec. 3. We explore dependencies on various experimentally controllable parameters and discuss the relation of our results to previous work. Our conclusions are given in Sec. 4.

2. Theoretical method

2.1. Fluctuating gap model

Quantum (and classical) systems experience dissipation and fluctuations through interaction with a reservoir or environment [18]. Here, the hydrogenization of the graphene sample induces states, which we consider as a reservoir. The interaction with the states of the reservoir generates fluctuation, and a short explanation of the technical details is given in Appendix A. In the

context of the open quantum system (subsystem and reservoir), we consider the tight-binding Hamiltonian for electrons in graphene subject to a sublattice-staggered potential,

$$\hat{\mathcal{H}} = -t \sum_{\langle i,j \rangle, s} (\hat{a}_{i,s}^\dagger \hat{b}_{j,s} + H.C.) + \sum_{i,s} V_{i,a} \hat{a}_{i,s}^\dagger \hat{a}_{i,s} + \sum_{i,s} V_{i,b} \hat{b}_{i,s}^\dagger \hat{b}_{i,s}, \quad (1)$$

where $\hat{a}_{i,s}^\dagger$, $\hat{a}_{i,s}$ annihilates (creates) an electron with spin s ($s = \uparrow, \downarrow$) on site i on sublattice A (an equivalent definition is used for $\hat{b}_{i,s}^\dagger$, $\hat{b}_{i,s}$ on sublattice B), $t \approx 2.8\text{eV}$ is the nearest-neighbor hopping energy between different sublattices. $V_{i,a}$ and $V_{i,b}$ are spin-independent potentials with $V_{i,a} = m_i$ on sublattice A and $V_{i,b} = -m_i$ on sublattice B . These potentials break the sublattice symmetry of the single-layer graphene.

As a consequence of the interaction with the reservoir, m_i is a time-dependent random variable at lattice site i , having a mean value $\langle\langle m_i(t) \rangle\rangle = \bar{m}$ and a variance $\langle\langle (m_i(t) - \bar{m})(m_j(t') - \bar{m}) \rangle\rangle = g^2 \delta_{i,j} \delta(t - t')$. The double expectation value is just the average over the local probability distribution function related to the lattice site i , followed by averaging over the whole lattice probability distribution function. In a more general case [24], values for $m_i(t)$ at different lattice sites could be correlated. We make the assumption that the random variables are uncorrelated for different lattice sites and the value of the average gap (averaging locally) is the same for each lattice site. This random-mass variable can be modeled as $m_i(t) = \bar{m} + g\xi_i(t)$, where $\xi_i(t)$ represents temporal white-noise fluctuation at lattice site i , and $\langle\langle \xi_i(t) \xi_j(t') \rangle\rangle = \delta_{i,j} \delta(t - t')$.

We remind the reader that the static disorder models discuss only spatial correlations between different lattice sites. The aforementioned description given by us could deal with local (temporal fluctuations) and spatial correlations, too. However, in the present paper we consider a complementary case to the static disorder models. Our model for randomness is given by the relation $m_i(t) = \bar{m} + g\xi_i(t)$, and it is clear that an average over the local fluctuations leads to a spatially uncorrelated variable \bar{m} .

The usual derivation [7] of the low-energy continuum model for quasiparticles in graphene yields the Hamiltonian

$$\hat{H}(\mathbf{k}) = \hbar v (\sigma_x \hat{\mathbf{k}}_x + \sigma_y \hat{\mathbf{k}}_y) + m(t) \sigma_z \hat{\mathbf{1}}_{\mathbf{k}}, \quad (2)$$

with multiplication operators $\hat{\mathbf{k}}_x$, $\hat{\mathbf{k}}_y$, $\hat{\mathbf{1}}_{\mathbf{k}}$ (that become numbers $k_x, k_y, 1$ in the plane-wave representation), and σ_i denoting the Pauli matrices for the pseudo-spin degree of freedom. v is the Fermi velocity, which has a value $\simeq 10^6$ m/s. The $m(t)$ represents the randomness introduced in the tight-binding model; it is equal to $\bar{m} + g\xi(t)$, where $\xi(t)$ is the usual white noise. The white noise, $\xi(t)$, dependence on the $\xi_j(t)$ is defined by $\sum_j \xi_j(t) e^{i(\mathbf{k}' - \mathbf{k}) \cdot \mathbf{R}_j} = \xi(t) \delta(\mathbf{k}' - \mathbf{k})$, where \mathbf{k}, \mathbf{k}' are the variables of the Fourier transformation, and \mathbf{R}_j is the position vector of lattice site j .

We assume disorder potentials to be weak (inducing small momentum scattering) such that the inequivalent Dirac points associated with the \mathbf{K} and \mathbf{K}' valleys in graphene's band structure are uncoupled [25] and, thus, contribute additively to electronic transport. This allows us to consider the presence of randomness for each valley separately. The fact that electrons in graphene also carry a real spin introduces an additional double degeneracy of all eigenvalues for the Hamiltonian (2). In the following, we study the dynamics due to the single-valley, spin-less model defined by Eq. (2) and absorb degeneracy factors into our basic unit of conductivity.

2.2. Quantum-stochastic time evolution for the density matrix

As the Hamiltonian (2) contains a random variable, the time evolution induced by it cannot be expressed by the usual equations. Instead, a quantum-stochastic calculus has to be applied. A brief

introduction to that is presented in the following. [26, 27] An isolated quantum system evolves in a unitary fashion. A physical quantity that is given at time $t = 0$ by an observable \hat{A} , will be described at time $t > 0$ by $\hat{A}(t) = \hat{U}^\dagger(t)\hat{A}\hat{U}(t)$, where $\hat{U}(t)$ is a unitary operator for each point in time t . The unitary operator is generated by the Schrödinger equation:

$$\frac{d\hat{U}(t)}{dt} = -\frac{i}{\hbar}\hat{H}_0(t)\hat{U}(t), \quad (3)$$

where the (time dependent) Hamiltonian $\hat{H}_0(t)$ is a self-adjoint operator for each t . The Schrödinger equation tells us that in a short time interval dt , the unitary operator changes at time t like

$$d\hat{U}(t) = -\frac{i}{\hbar}\hat{H}_0(t)\hat{U}(t)dt. \quad (4)$$

The Hamiltonian in Eq. (2) can be written in the form of $\hat{H}(\mathbf{k}) = \hat{H}_0(\mathbf{k}) + \hat{H}_1\xi(t)$, where

$$\hat{H}_0(\mathbf{k}) = \hbar v(\sigma_x\hat{\mathbf{k}}_x + \sigma_y\hat{\mathbf{k}}_y) + \bar{m}\sigma_z\hat{\mathbf{1}}_{\mathbf{k}}, \quad (5a)$$

$$\hat{H}_1 = g\sigma_z\hat{\mathbf{1}}_{\mathbf{k}}. \quad (5b)$$

The white noise $\xi(t)$ is the formal derivative of a Wiener process W_t (continuous everywhere but differentiable nowhere), a Gaussian random variable with zero mean value

$$\mathbf{M}(W_t) = 0, \quad (6)$$

and variance t

$$\mathbf{M}(W_t^2) - \mathbf{M}(W_t)^2 = t. \quad (7)$$

The stochastic calculus applied here will be based on the Wiener process W_t . The above properties are represented in the differential equations as

$$\mathbf{M}(dW_t) = 0, \quad d^2W_t = dt, \quad d^nW_t = 0, \quad n > 2, \quad (8)$$

all of which will be applied in further calculations. Consider a stochastic processes X_t governed by a stochastic differential equations

$$dX_t = V_x dt + D_x dW_t,$$

where physical meaning of V_x is the drift and of D_x is the diffusion. The Ito rule for a smooth function $f(x)$ states:

$$\begin{aligned} df(X_t) &= f'(X_t)dX_t + \frac{1}{2}f''(X_t)(dX_t)^2, \\ f'(x) &= \frac{df(x)}{dx}, \quad f''(x) = \frac{d^2f(x)}{dx^2}, \quad x \in \mathbb{R}, \\ (dX_t)^2 &= D_x^2 dt. \end{aligned}$$

The quantum Ito rule [28] is the same as the Ito rule, only the noncommutativity of the operators is considered in addition.

Now, we apply the properties of the stochastic calculus, and we see that the unitary operator changes within an infinitesimal short time interval dt at time t as follows:

$$d\hat{U}(t) = \left(-\frac{i}{\hbar}\hat{H}_0(\mathbf{k})dt - \frac{1}{2\hbar^2}\hat{H}_1^2 dt - \frac{i}{\hbar}\hat{H}_1 dW_t \right) \hat{U}(t). \quad (9)$$

The equation of motion of the density matrix is given by $\hat{\rho}(t) = \hat{U}(t)\hat{\rho}\hat{U}^\dagger(t)$, and a straightforward calculation yields

$$d\hat{\rho}(t) = -\frac{i}{\hbar}[\hat{H}_0(\mathbf{k}), \hat{\rho}(t)]dt - \frac{1}{2\hbar^2}[\hat{H}_1, [\hat{H}_1, \hat{\rho}(t)]]dt - \frac{i}{\hbar}[\hat{H}_1, \hat{\rho}(t)]dW_t. \quad (10)$$

The current operator in our system is defined by $\hat{j}_\mu = e\frac{d\hat{r}_\mu}{dt}$, where the time evolution of the coordinate operator satisfies

$$d\hat{r}_\mu(t) = \frac{i}{\hbar}[\hat{H}_0(\mathbf{k}), \hat{r}_\mu(t)]dt - \frac{1}{2\hbar^2}[\hat{H}_1, [\hat{H}_1, \hat{r}_\mu(t)]]dt + \frac{i}{\hbar}[\hat{H}_1, \hat{r}_\mu(t)]dW_t. \quad (11)$$

\hat{r}_μ is a derivative operator in the \mathbf{k} -space and, in the sublattice representation, is given by $\hat{\mathbf{1}}_2 \otimes i\frac{\partial}{\partial k_\mu}$. This operator commutes with \hat{H}_1 , which has a structure of $\sigma_z \otimes \hat{\mathbf{1}}_k$. These conditions and Eq. (11) define the current operator as $\hat{j}_\mu = \frac{ie}{\hbar}[\hat{H}_0(\mathbf{k}), \hat{r}_\mu] = \frac{e}{\hbar}\frac{\partial \hat{H}_0(\mathbf{k})}{\partial k_\mu}$. Due to the operator structure in Eq. (2), the single-particle eigenstates $|n\rangle$ of this model can be written as a direct product of a plane wave in configuration space with a spinor: $|n\rangle = |\mathbf{k}\rangle \otimes |\pm\rangle_{\mathbf{k}}$ [8, 29]. Here \pm labels the electron and hole bands, respectively, and the spinor wave function depends on wave vector \mathbf{k} . The Cartesian current components are $\hat{j}_x = ev\sigma_x$ and $\hat{j}_y = ev\sigma_y$ [30]. The definition of the equilibrium density matrix in the spinor space is $\hat{\rho}_0|\pm\rangle_{\mathbf{k}} = f(\epsilon_{\mathbf{k},\pm})|\sigma\rangle_{\mathbf{k}}$, and $\hat{H}_0|\pm\rangle_{\mathbf{k}} = \epsilon_{\mathbf{k},\pm}|\pm\rangle_{\mathbf{k}}$, where f is the Fermi-Dirac distribution function and $\epsilon_{\mathbf{k},\pm} = \pm\sqrt{(\hbar v)^2|\mathbf{k}|^2 + \bar{m}^2}$. This equilibrium state is the average of all equilibrium realizations defined by $\hat{\rho}_0 = e^{-\beta\hat{H}(\mathbf{k})}/\text{Tr}(e^{-\beta\hat{H}(\mathbf{k})})$.

2.3. Generalization of linear-response formalism

We employ the linear-response (Kubo) formalism [31] and divide the system's Hamiltonian into the part $\hat{H}(\mathbf{k})$, which governs the evolution in Eq. (10), and $\delta\hat{H}$, the perturbation associated with an external electric field \mathbf{E} . For simplicity, we take the latter to be constant in space and assume the field to be applied between $t = -\infty$ and $t = 0$. The perturbation Hamiltonian is $\delta\hat{H} = -e\mathbf{E} \cdot \hat{\mathbf{r}} e^{i\omega t}$. The equation of motion of the system with the added external field is:

$$\begin{aligned} d\hat{\rho}(t) &= -\frac{i}{\hbar}[\hat{H}_0(\mathbf{k}), \hat{\rho}(t)]dt - \frac{i}{\hbar}[\delta\hat{H}, \hat{\rho}(t)]dt - \frac{1}{2\hbar^2}[\hat{H}_1, [\hat{H}_1, \hat{\rho}(t)]]dt - \frac{i}{\hbar}[\hat{H}_1, \hat{\rho}(t)]dW_t \\ &= \mathcal{L}\hat{\rho}(t)dt - \frac{i}{\hbar}[\delta\hat{H}, \hat{\rho}(t)]dt - \frac{i}{\hbar}[\hat{H}_1, \hat{\rho}(t)]dW_t. \end{aligned}$$

Within linear-response theory, we can linearize $\hat{\rho} = \hat{\rho}_0 + \delta\hat{\rho}$, where $\hat{\rho}_0$ is the system's equilibrium density matrix. Keeping only linear terms in Eq. (12), we get

$$d\delta\hat{\rho} = \mathcal{L}\delta\hat{\rho}dt - \frac{i}{\hbar}[\delta\hat{H}, \hat{\rho}_0]dt - \frac{1}{2\hbar^2}[\hat{H}_1, [\hat{H}_1, \hat{\rho}_0]]dt - \frac{i}{\hbar}[\hat{H}_1, \hat{\rho}_0 + \delta\hat{\rho}]dW_t, \quad (12)$$

with using $[\hat{H}_0(\mathbf{k}), \hat{\rho}_0] = 0$ as well as $[\delta\hat{H}, \delta\hat{\rho}] \simeq 0$. Introducing $\Delta\hat{\rho} = e^{-\mathcal{L}t}\delta\hat{\rho}$ yields

$$d\Delta\hat{\rho} = e^{-\mathcal{L}t}\left(-\frac{i}{\hbar}[\delta\hat{H}, \hat{\rho}_0] - \frac{1}{2\hbar^2}[\hat{H}_1, [\hat{H}_1, \hat{\rho}_0]]\right)dt - \frac{i}{\hbar}e^{-\mathcal{L}t}\left([\hat{H}_1, \hat{\rho}_0 + e^{\mathcal{L}t}\Delta\hat{\rho}]\right)dW_t. \quad (13)$$

Note that $\Delta\hat{\rho}$ and $\delta\hat{\rho}$ have the same value at $t = 0$, and both vanish at $t = -\infty$. Integration yields

$$\delta\hat{\rho}(t=0) = \int_{-\infty}^0 dt e^{-\mathcal{L}t}\left(-\frac{i}{\hbar}[\delta\hat{H}, \hat{\rho}_0] - \frac{1}{2\hbar^2}[\hat{H}_1, [\hat{H}_1, \hat{\rho}_0]]\right) + \lim_{t \rightarrow \infty} \int_{-t}^0 dW_t \left(e^{-\mathcal{L}t}\left(\frac{i}{\hbar}[\hat{H}_1, \hat{\rho}_0]\right) - \frac{i}{\hbar}[\hat{H}_1, \Delta\hat{\rho}]\right). \quad (14)$$

The exponential factor in Eq. (14) ensures convergence of the time integral, making it unnecessary to introduce the phenomenological adiabatic damping parameter employed in conventional linear-response theory [31].

2.4. Generalized conductivity formula

We use (14) to calculate the double expectation value (over the basis of the one-particle Hilbert space and over the ensemble of realizations for the stochastic process) for the current operator \hat{j} and use the property $\mathbf{M}(dW_t) = 0$. We remind the reader that our stochastic variable models the local gap fluctuations. An average over this randomness yields the mean conductivity [32] that is typically calculated and is our quantity of interest here. Dividing the current expectation value by $|\mathbf{E}|$ yields the optical conductivity

$$\sigma_{\mu\nu}(\omega) = \int_{-\infty}^0 [K_{\mu\nu}(t)e^{i\omega t} + L_{\mu\nu}(t)] dt, \quad (15)$$

with the kernels

$$K_{\mu\nu}(t) = -\frac{1}{i\hbar} \text{Tr} \left\{ \hat{j}_\mu e^{-\mathcal{L}t} ([e\hat{r}_\nu, \hat{\rho}_0]) \right\}, \quad (16)$$

$$L_{\mu\nu}(t) = \text{Tr} \left\{ \frac{\hat{j}_\mu}{E_\nu} e^{-\mathcal{L}t} \left(-\frac{1}{2\hbar^2} [\hat{H}_1, [\hat{H}_1, \hat{\rho}_0]] \right) \right\}. \quad (17)$$

The Tr symbol stands for taking the trace over 2×2 matrices and performing the integration $\int d^2\mathbf{k}$. As the integrand in Eq. (17) is an odd function of both k_x and k_y , the integration over the polar angle yields zero and, hence, the quantity $L_{\mu\nu}(t)$ vanishes.

We remind the reader that the current flowing through the system was not affected by the fluctuations, see Eq. (11) and the discussion afterwards. Otherwise, the variance of the fluctuations must be added to the conductivity formula. This constant would shift the universal conductance of the graphene sheet, and would refute the experimental results. This is not the situation here, which shows the correctness of our model.

The calculation of $K_{\mu\nu}$ is straightforward, and using the Laplace transform to solve for the dynamics, we find

$$K_{\mu\nu}(t) = \frac{e^2}{\hbar} \int \frac{d^2\mathbf{k}}{(2\pi)^2} \mathbf{Res} \left\{ \frac{N(\mathbf{k}, \bar{m}, g, z)}{D(\mathbf{k}, \bar{m}, g, z)} e^{zt} \right\}, \quad (18)$$

where \mathbf{Res} stands for the sum of residues of the integrand. The conductivities related to the kernels K_{xx} and K_{yy} are identical, and we present the effect of the fluctuating gap for these particular conductivities. We have to mention that the Hall conductivities σ_{xy} and σ_{yx} are equal to zero, even in the presence of the fluctuations. Without an external magnetic field, the contribution of the two valleys of the honeycomb-lattice band-structure cancel each other.

Introducing polar coordinates for \mathbf{k} and performing the angular integration yields

$$K_{\mu\nu}(t) = \frac{e^2}{\hbar} \int_0^\infty \frac{|\mathbf{k}| d|\mathbf{k}|}{4\pi} \mathbf{Res} \left\{ \frac{N(|\mathbf{k}|, \bar{m}, g, z)}{D(|\mathbf{k}|, \bar{m}, g, z)} e^{zt} \right\}. \quad (19)$$

For simplicity, the Fermi velocity v has been absorbed into $|\mathbf{k}|$, and we find

$$\begin{aligned} N(|\mathbf{k}|, \bar{m}, g, z) &= |\mathbf{k}|^2 \sqrt{m^2 + |\mathbf{k}|^2} (4m^2 + 4|\mathbf{k}|^2 + z^2 - 4\Gamma z) \times \sum \left(-\frac{df(\epsilon)}{d\epsilon} \Big|_{\epsilon=\epsilon_{\mathbf{k},\pm}} \right) \\ &+ z(z - 4\Gamma)(2m^2 + |\mathbf{k}|^2) [f(\epsilon_{\mathbf{k},-}) - f(\epsilon_{\mathbf{k},+})], \end{aligned} \quad (20)$$

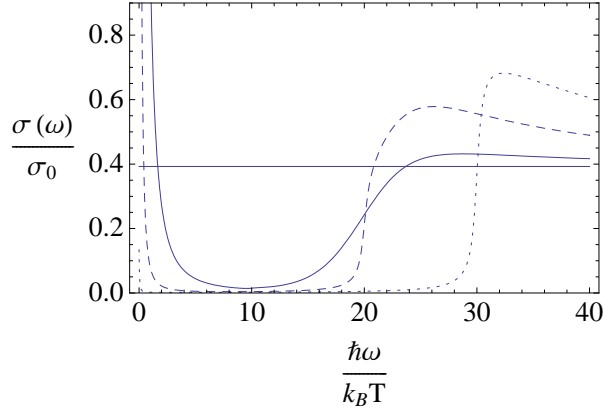


Figure 1: Optical conductivity of single-layer graphene with a weakly fluctuating mass gap. Results shown are obtained for fixed chemical potential $\mu = 10 k_B T$ and gap-fluctuation variance $\hbar\Gamma = 0.1 k_B T$. The different curves correspond to $\bar{m}/k_B T = 5$ (solid), $\bar{m}/k_B T = 10$ (dashed), and $\bar{m}/k_B T = 15$ (dotted). The value of $\pi/8$ is marked by a horizontal line. As can be seen, the ac conductivity exhibits a jump at twice the average band-gap value \bar{m} when the latter is greater than or equal to the chemical potential.

$$D(|\mathbf{k}|, \bar{m}, g, z) = (m^2 + |\mathbf{k}|^2)^{\frac{3}{2}} \left[16z\Gamma^2 - 8(2|\mathbf{k}|^2 + z^2)\Gamma + z(4m^2 + 4|\mathbf{k}|^2 + z^2) \right], \quad (21)$$

where the parameters $\Gamma = g^2/2\hbar^2$ and $m = \bar{m}/\hbar$ have been introduced. The cubic factor in the denominator (21) has three roots z_i , which give the poles in eq. (19).

3. Optical conductivity of gapped graphene

For small Γ , the roots are to lowest order $z_1 = 0$ and $z_{2,3} = \pm 2i\sqrt{|\mathbf{k}|^2 + m^2}$. Using this and performing the time-integration in the limit $\Gamma \rightarrow 0$, the *intra*-band contribution

$$\frac{\sigma}{\sigma_0} = \frac{\pi}{2} \delta(\omega) \int_0^\infty \frac{|\mathbf{k}|^3}{m^2 + |\mathbf{k}|^2} \sum \left(-\frac{df(\epsilon)}{d\epsilon} \Big|_{\epsilon=\epsilon_{\mathbf{k},\pm}} \right) d|\mathbf{k}|, \quad (22)$$

and the *inter*-band contribution

$$\frac{\sigma(\omega)}{\sigma_0} = \frac{\pi}{8} \frac{\omega^2 + 4m^2}{\omega^2} \frac{\sinh(\frac{\hbar\omega}{2k_B T})}{\cosh(\frac{\mu}{k_B T}) + \cosh(\frac{\hbar\omega}{2k_B T})} \Theta(\omega - 2m), \quad (23)$$

to the conductivity of the uniformly gapped single-layer graphene are found [23]. The Dirac-delta peak in the *intra*-band conductivity is due to elastic transitions, which are only possible at finite temperature and/or when the chemical potential is bigger than the average gap. The scale factor $\sigma_0 = 4e^2/h$ accounts for spin and valley degeneracy.

In the following, the conductivity is calculated numerically for finite values of Γ and T from Eq. (15) with Eq. (19). We use $k_B T$ as our unit of energy. Figs. 1 and 2 show the ac (optical) conductivity, whereas Figs. 3, 4 and 5 show results for the dc conductivity.

The interplay between average-gap size and chemical potential exhibits two regimes, as can be seen by studying the uniform gapped model [result given by Eq. (23)] and also from Fig. 1.

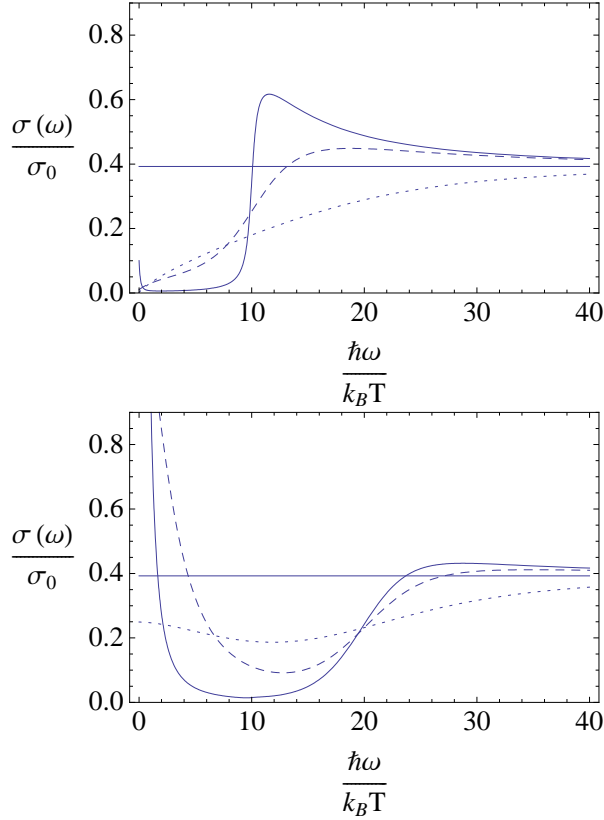


Figure 2: Optical conductivity of single-layer graphene with a fluctuating gap. Top panel: the chemical potential is fixed at the neutrality point ($\mu/k_B T = 0$), and the average gap is $\bar{m}/k_B T = 5$. Bottom panel: $\mu = 10 k_B T$ and $\bar{m} = 5 k_B T$. The different curves correspond to $\hbar\Gamma/k_B T = 0.1$ (solid), $\hbar\Gamma/k_B T = 1$ (dashed), and $\hbar\Gamma/k_B T = 5$ (dotted). The value of $\pi/8$ is marked by the horizontal line. As the value of Γ is decreased, the curves resemble more closely the result found for uniformly gapped graphene. Note the intermediate range of low frequencies where an increase in randomness (i.e., variance of fluctuations) results in an enhanced conductivity.

The uniform gap model has a vanishing ac conductivity for photon energies $\hbar\omega < 2\bar{m}$, and a jump at $\hbar\omega = 2\bar{m}$. The height of the jump depends on the chemical potential and the average gap. If the chemical potential is much bigger than the average gap then we have a small jump height whereas, in the opposite case, the jump is more noticeable. The ability to determine the average gap size by measuring where the jump of the optical conductivity occurs depends also on the variance of the fluctuations. In any case, setting the chemical potential as low as possible would be favorable for the detection of the gap-induced jump in the ac conductivity.

Figure 2 shows the ac conductivity for a number of different variances of gap fluctuations for two values of the chemical potential μ : tuned to the neutrality point (top panel) and for a large value of μ (bottom panel). While the situation with a small variance of gap fluctuations is quite similar to the result found for a system with a uniform gap, the increase of fluctuations generates sizable conduction in the frequency range $\omega < 2\bar{m}$. For both values of the chemical potential, a region emerges where an increase in fluctuations results in an increased conductivity. Thus

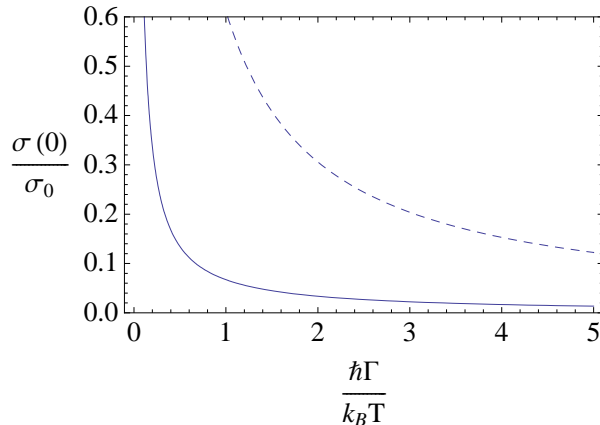


Figure 3: The dc conductivity of randomly gapped graphene plotted as a function of gap variance Γ . The average gap is fixed at $\bar{m}/k_B T = 2.5$. The different curves are for $\mu/k_B T = 0$ (solid) and $\mu/k_B T = 5$ (dashed). A decrease in the dc conductivity is found for increasing Γ . This decrease is slower when the chemical potential is bigger than the average gap.

it appears that larger fluctuations will facilitate electric transport in randomly gapped graphene sheets. A similar result has been reported for static random-gap disorder in graphene [15, 17]. However, in our case, this behavior occurs only within a limited range of finite frequencies. The parametric dependence on the fluctuation strength is reversed at low frequencies, in particular also for the dc conductivity. For high frequencies, the conductivity approached the universal value $\pi/8$. The detailed shape of the saturation depends on both Γ and \bar{m} , with higher values pushing convergence to higher frequencies.

The dc conductivity's dependence on the parameters Γ , \bar{m} , and the chemical potential is shown by Figs. 3, 4 and 5. Increasing Γ leads to a decrease in the dc conductivity, which means that the Γ simulate the same effect as life-time broadening due to inelastic scattering. The rate of the decrease depends on the relative magnitudes of μ and \bar{m} , as can be seen in Fig. 3. If the chemical potential is bigger than the average gap, the dc conductivity tends to zero slower with any increase of Γ . Increasing the average gap also leads to a decrease in the dc conductivity. The minimal value of the dc conductivity occurs at the charge neutrality point, $\mu = 0$, and strongly depends on the value of Γ and \bar{m} .

Up until now, we considered electron transport at a finite temperature. To discuss the behavior in the limit when $T \rightarrow 0$, we have to perform this limit already in Eq. (19) and redo the calculations following after that. In the case of $T \rightarrow 0$ and $\mu = 0$ we are able to compare our results to the works by Ziegler [15]. These works assume that the static disorder average destroys the intra-band conductivity, which we also found for the above assumptions. We are able to go further and in the case of $T \rightarrow 0$ and $\mu \leq \bar{m}$ the intra-band conductivity is still found to be zero. In the analytical works by Ziegler [15], the inter-band conductivity contains a Heaviside function and has a contribution at $\omega = 0$. The role of the Heaviside function is to separate the insulating regime from the metallic one. This is a point where we have a significant difference, because our Heaviside function is smeared by the Γ parameter. In the limit $\omega = 0$ with $\bar{m} \neq 0$ and $\mu \leq \bar{m}$, our inter-band conductivity is always zero.

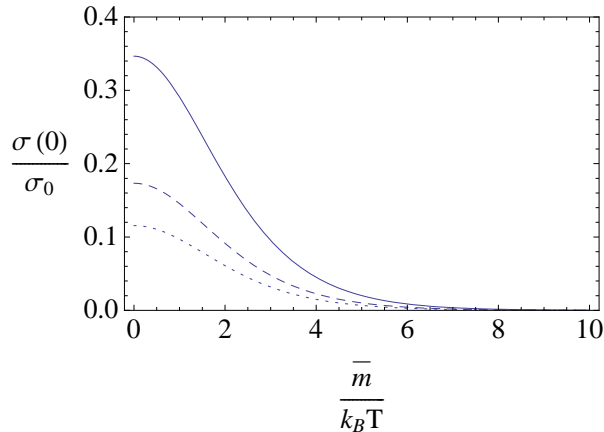


Figure 4: The dc conductivity of randomly gapped graphene plotted as a function of average gap for different values of gap variance Γ . The different curves correspond to $\hbar\Gamma/k_B T = 0.5$ (solid), $\hbar\Gamma/k_B T = 1$ (dashed), and $\hbar\Gamma/k_B T = 1.5$ (dotted). The chemical potential is fixed at the neutrality point. As the average gap size is increased, the dc conductivity gets suppressed.

The role played by the quantity Γ in the present work is formally similar to a decoherence parameter (also denoted by Γ in a previous work [33] by us) measuring the effect of an ever-present environment. The parameter Γ is the coefficient of a double commutator that enters to the system's time evolution. In the present case, the double commutator contains the $\hat{\sigma}_z$ operator, in contrast to our previous work [33] where it involved the $\hat{\sigma}_x$ and $\hat{\sigma}_y$ matrices. The physical meaning of Γ is also different: here it is related to the randomness of a mass-gap-inducing degree of freedom such as hydrogen atoms, while it was used to describe the properties of a current detector previously. We would also like to point out that, in general, the gap fluctuations could be temperature-dependent, as most mechanisms for inducing a gap (e.g., by structural modifications such as hydrogenation) will be affected by a variation of temperature. As we have introduced the fluctuating gap in a phenomenological fashion, our theory would apply to the ensemble of temporal fluctuations at a fixed temperature.

4. Conclusions

We have calculated the stochastic evolution of the density matrix for charge-carrier dynamics in single-layer graphene subject to a fluctuating sublattice-staggered potential. We derived a generalized Kubo formula to study the effect of temporal mass-gap fluctuations on the conductivity. The variance of the fluctuations introduces a source of damping and thus makes the converged adiabaticity parameter frequently used in Kubo formula calculations superfluous. See also related work [33]. Mixing of the *intra*-band and *inter*-band contributions to the ac and dc conductivities strongly affect its parametric dependence on the variance of the fluctuations $g^2 = 2\hbar^2\Gamma$. A system with a uniform gap (i.e., vanishing variance Γ) is insulating, as seen from Eq. (23). For the more realistic case of a fluctuating gap, a finite range of frequencies is found for which an increase in randomness (i.e., variance of gap fluctuations) results in an increase of the ac conductivity. See Fig. 2. Such fluctuation-enhanced transport is not observed in the dc limit,

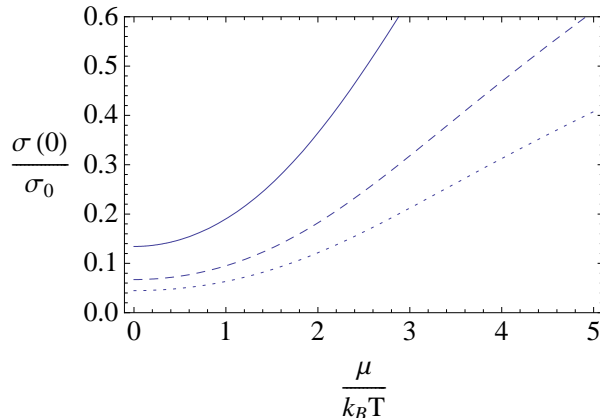


Figure 5: The dc conductivity of randomly gapped graphene, plotted as a function of chemical potential for different values of gap variance Γ . The different curves were obtained for $\hbar\Gamma/k_B T = 0.5$ (solid), $\hbar\Gamma/k_B T = 1$ (dashed), and $\hbar\Gamma/k_B T = 1.5$ (dotted). The average gap is fixed at $\bar{m}/k_B T = 2.5$. The minimal value of the dc conductivity occurs at $\mu = 0$ and decreases with increasing Γ .

where increases in either the average size or the variance of the mass gap lead to a suppression of conductivity at any finite temperature. In the zero-temperature limit, our model of randomly gapped graphene exhibits insulating behavior when the average gap is finite [14, 16] (but, as in the previous work [14], a finite dc conductivity is found when the average gap vanishes).

The discussed differences between different random gap models can be found out in the properties of the conductivity, the only quantity retained after a measurement.

The author has profited from helpful discussion with K. Ziegler, A. Sinner and U. Zülicke. This work was supported by a postdoctoral fellowship grant from the Massey University Research Fund. Additional funding through BMBF project QK_QuOReP is gratefully acknowledged.

Appendix A. Stochastic dynamics

A quantum master equation describes the dynamics of an open quantum system (subsystem+reservoir). The Markovian quantum master equation is given by a first-order differential equation for the density matrix of the subsystem,

$$\frac{d}{dt}\hat{\rho}_S(t) = \mathcal{L}\hat{\rho}_S(t), \quad (\text{A.1})$$

where the most general form for the generator \mathcal{L} is given by the Lindblad equation [34, 35],

$$\mathcal{L}\hat{\rho}_S = -\frac{i}{\hbar}[\hat{H}_S, \hat{\rho}_S] + \sum_k \gamma_k \left(\hat{A}_k \hat{\rho}_S \hat{A}_k^\dagger - \frac{1}{2} \hat{A}_k^\dagger \hat{A}_k \hat{\rho}_S - \frac{1}{2} \hat{\rho}_S \hat{A}_k^\dagger \hat{A}_k \right). \quad (\text{A.2})$$

The first term of the generator represents the unitary part of the dynamics generated by the Hamiltonian \hat{H}_S of the subsystem. The operators \hat{A}_k are the Lindblad operators and the quantities

γ_k have the dimension of an inverse time. The operators \hat{A}_k and the quantities γ_k are derived from the dynamics of the total system (subsystem and reservoir) in various approximation schemes. The states of the reservoir are traced out during the procedure.

It is clear that the eq. (A.1) cannot be used for the derivation elaborated in the work of Semenoff [7]. The master equation for the subsystem can be reformulated in terms of a stochastic process for the subsystem's wave function. This idea is the so-called *unravelling* of the master equation [36, 37].

Now, we consider our microscopic model of the total system,

$$\begin{aligned}\hat{H} &= \hat{H}^g + \hat{H}_I + \hat{H}^r, \\ \hat{H}^g &= -t \sum_{\langle i,j \rangle, s} (\hat{a}_{i,s}^\dagger \hat{b}_{j,s} + H.C.) + \sum_{i,s} \bar{m}_i \hat{a}_{i,s}^\dagger \hat{a}_{i,s} - \sum_{i,s} \bar{m}_i \hat{b}_{i,s}^\dagger \hat{b}_{i,s}, \\ \hat{H}_I &= \sum_{i,s} \lambda_i \hat{a}_{i,s}^\dagger \hat{a}_{i,s} \otimes \hat{H}_{I,i,s,a}^r - \sum_{i,s} \lambda_i \hat{b}_{i,s}^\dagger \hat{b}_{i,s} \otimes \hat{H}_{I,i,s,b}^r,\end{aligned}\quad (\text{A.3})$$

where $\hat{a}_{i,s}^\dagger$, $\hat{a}_{i,s}$ annihilates (creates) an electron with spin s ($s = \uparrow, \downarrow$) on site i on sublattice A (an equivalent definition is used for $\hat{b}_{i,s}^\dagger$, $\hat{b}_{i,s}$ on sublattice B). \hat{H}^r is the Hamiltonian of the states, considered as reservoir. \hat{H}_I is the interaction Hamiltonian and $\hat{H}_{I,i,s,a}^r$ and $\hat{H}_{I,i,s,b}^r$ are functions of creation and annihilation operators related to the states of the reservoir coupled to sublattices A and B . The interaction Hamiltonian is chosen such that the sublattice symmetry is broken. λ_i is a spin independent coupling constant. \bar{m}_i is the strength of the sublattice symmetry breaking on lattice site i .

The usual Born-Markov master equation [27] can be derived by considering that the time scale of the hopping is much more faster than the relaxation of the reservoir states and the couplings are weak:

$$\frac{d\hat{\rho}_S}{dt} = \mathcal{L}\hat{\rho}(t) = -\frac{i}{\hbar}[\hat{H}^g, \hat{\rho}_S(t)] - \frac{1}{\hbar^2} \int_0^t \text{Tr}_r [\hat{H}_I(t), [\hat{H}_I(s), \hat{\rho}_S(t) \otimes \hat{\rho}_r]] ds, \quad (\text{A.4})$$

where Tr_r stands for the partial trace over the reservoir states. $\hat{\rho}_r$ is the density matrix of the reservoir. Inserting Eq. (A.3) into the master equation (Eq. (A.4)) we obtain

$$\begin{aligned}\frac{d\hat{\rho}_S}{dt} &= -\frac{i}{\hbar}[\hat{H}^g, \hat{\rho}_S(t)] - \frac{1}{\hbar^2} \sum_{i,s} \frac{g_i^2}{2} [\hat{H}_I^g, [\hat{H}_I^g, \hat{\rho}_S(t)]], \\ \hat{H}_I^g &= \hat{a}_{i,s}^\dagger \hat{a}_{i,s} - \hat{b}_{i,s}^\dagger \hat{b}_{i,s},\end{aligned}\quad (\text{A.5})$$

where g_i is related to the reservoir correlation functions, and we considered that these correlations are the same for sublattice A and B , too.

The *unravelling* of the above master equation gives the following stochastic Hamiltonian

$$\hat{H} = -t \sum_{\langle i,j \rangle, s} (\hat{a}_{i,s}^\dagger \hat{b}_{j,s} + H.C.) + \sum_{i,s} \bar{m}_i(t) \hat{a}_{i,s}^\dagger \hat{a}_{i,s} - \sum_{i,s} \bar{m}_i(t) \hat{b}_{i,s}^\dagger \hat{b}_{i,s}, \quad (\text{A.6})$$

where

$$\bar{m}_i(t) = \bar{m}_i + g_i \xi(t). \quad (\text{A.7})$$

$\xi(t)$ stands for the standard white noise.

References

- [1] K. S. Novoselov, A. K. Geim, S. V. Morozov, D. Jiang, Y. Zhang, S. V. Dubonos, I. V. Grigorieva, and A. A. Firsov, *Science* **306**, 666 (2004).
- [2] K. S. Novoselov, D. Jiang, T. Booth, V. V. Khotkevich, S. M. Morozov, and A. K. Geim, *PNAS* **102**, 10451 (2005).
- [3] A. K. Geim and K. S. Novoselov, *Nat. Mater.* **6**, 183 (2007).
- [4] A. K. Geim, *Science* **324**, 1530 (2009).
- [5] P. R. Wallace, *Phys. Rev.* **71**, 622 (1947).
- [6] J. C. Slonczewski and P. R. Weiss, *Phys. Rev.* **109**, 272 (1958).
- [7] G. W. Semenoff, *Phys. Rev. Lett.* **53**, 2449 (1984).
- [8] A. H. Castro Neto, F. Guinea, N. M. R. Peres, K. S. Novoselov, and A. K. Geim, *Rev. Mod. Phys.* **81**, 109 (2009).
- [9] S. V. Morozov, K. S. Novoselov, M. I. Katsnelson, F. Schedin, D. C. Elias, J. A. Jaszczak, and A. K. Geim, *Phys. Rev. Lett.* **100**, 016602 (2008).
- [10] J.-H. Chen, C. Jang, S. Xiao, M. Ishigami, and M. S. Fuhrer, *Nat. Nanotech.* **3**, 206 (2008).
- [11] Y. Zhang, J. P. Small, M. E. S. Amori, and P. Kim, *Phys. Rev. Lett.* **94**, 176803 (2005); Y. Zhang, Y. W. Tan, H. L. Stormer, and P. Kim, *Nature (London)* **438**, 201 (2005).
- [12] D. C. Elias, R. R. Nair, T. M. G. Mohiuddin, S. V. Morozov, P. Blake, M. P. Halsall, A. C. Ferrari, D. W. Boukhvalov, M. I. Katsnelson, A. K. Geim, and K. S. Novoselov, *Science* **323**, 610 (2009).
- [13] A. Bostwick, J. L. McChesney, K. V. Emtsev, T. Seyller, K. Horn, S. D. Kevan, and E. Rotenberg, *Phys. Rev. Lett.* **103**, 056404 (2009).
- [14] A. W. W. Ludwig, M. P. A. Fisher, R. Shankar, and G. Grinstein, *Phys. Rev. B* **50**, 7526 (1994).
- [15] K. Ziegler, *Phys. Rev. Lett.* **102**, 126802 (2009); *Phys. Rev. B* **79**, 195424 (2009).
- [16] J. H. Bardarson, M. V. Medvedyeva, J. Tworzyllo, A. R. Akhmerov, and C. W. J. Beenakker, *Phys. Rev. B* **81**, 121414(R) (2010).
- [17] K. Ziegler and A. Sinner, *Phys. Rev. B* **81**, 241404(R) (2010).
- [18] M. Lax, *Phys. Rev.* **145**, 110 (1966); H. Scher and M Lax, *Phys. Rev. B* **7**, 4491 (1973); H. Scher and M Lax, *Phys. Rev. B* **7**, 4502 (1973); C. W. Gardiner, *Handbook of Stochastic Processes* (Springer Verlag, Heidelberg and Berlin 1989); N. G. van Kampen, *Stochastic Processes in Physics and Chemistry* (North-Holland, Amsterdam 1981).
- [19] A. B. Kuzmenko, E. van Heumen, F. Carbone, and D. van der Marel, *Phys. Rev. Lett.* **100**, 117401 (2008).
- [20] K. F. Mak, M. Y. Sfeir, Y. Wu, C. H. Lui, J. A. Misewich, and T. F. Heinz, *Phys. Rev. Lett.* **101**, 196405 (2008).
- [21] F. Wang, Y. Zhang, C. Tian, C. Girit, A. Zettl, M. Crommie, and Y. R. Shen, *Science* **320**, 206 (2008).
- [22] Z. Q. Li, E. A. Henriksen, Z. Jiang, Z. Hao, M. C. Martin, P. Kim, H. L. Stormer, and D. N. Basov, *Nat. Phys.* **4**, 532 (2008).
- [23] V. P. Gusynin, S. G. Sharapov, and J. P. Carbotte, *Phys. Rev. Lett.* **96**, 256802 (2006); *New. J. Phys.* **11**, 095013 (2009).
- [24] As a simple example, but more general than the considered model in the main text, consider $m_i(t)$ given by $\bar{m}_i + g\xi_i(t)$: averaging first locally, we get $\langle m_i(t) \rangle_i = \bar{m}_i$ and then for the whole lattice system $\langle \bar{m}_i \rangle_N = \bar{m}$ is found. The variance $\langle (\bar{m}_i - \bar{m})(\bar{m}_j - \bar{m}) \rangle_N$ of the locally averaged variable \bar{m}_i is nonzero.
- [25] E. McCann, K. Kechedzhi, V. I. Falko, H. Suzuura, T. Ando, and B. L. Altshuler, *Phys. Rev. Lett.* **97**, 146805 (2006).
- [26] K. R. Parthasarathy, *An Introduction to Quantum Stochastic Calculus* (Birkhäuser, Basel 1992).
- [27] H.-P. Breuer and F. Petruccione, *The theory of open quantum systems* (Oxford University Press, Oxford 2002), chap. 6 and references therein.
- [28] R. L. Hudson and K. R. Parthasarathy, *Commun. Math. Phys.* **93**, 301 (1984).
- [29] J. Z. Bernad, U. Zülicke, and K. Ziegler, *Physica E* **42**, 755 (2010).
- [30] The Hilbert space is decomposed into irreducible components. Each pseudo-spin sector is a superselection sector, preserved by the current operator.
- [31] O. Madelung, *Introduction to Solid-State Theory* (Springer, Berlin, 1978).
- [32] A possible extension of this work is the full time dependence involving the Wiener process, which gives a picture of the raw measured data obtained for the conductivity.
- [33] J. Z. Bernad, M. Jääskeläinen, and U. Zülicke, *Phys. Rev. B* **81**, 073403 (2010).
- [34] G. Lindblad, *Commun. Math. Phys.* **40**, 147 (1976).
- [35] V. Gorini, A. Kossakowski, and E. C. G. Sudarshan, *J. Math. Phys.* **17**, 821 (1976).
- [36] E. B. Davies, *Commun. Math. Phys.* **15**, 277 (1969).
- [37] A. Barchielli and V. P. Belavkin, *J. Phys. A: Math. Gen.* **24**, 1495 (1991).